SEECCM III
3rd South-East European Conference on Computational Mechanics-
an ECCOMAS and IACM Special Interest Conference
M. Papadrakakis, M. Kojic, I. Tuncer (eds.)
Kos Island, Greece, 12–14 June 2013

STRUCTURAL AND MULTI-FUNCTIONAL OPTIMIZATION USING MULTIPLE PHASES AND A LEVEL-SET METHOD

G. Allaire[1], F. Jouve[2], and G. Michailidis[1,3]

[1]CMAP, Ecole Polytechnique
91128 Palaiseau, France
e-mail: gregoire.allaire@polytechnique.fr

[2] LJLL, University Paris Diderot
(UMR 7598), Paris, France
e-mail: jouve@math.jussieu.fr

[3] Renault DREAM-DELT'A
Guyancourt, France
e-mail: michailidis@cmap.polytechnique.fr

Keywords: Shape and topology optimization, multi-functional optimization, multi-materials, signed distance function.

Abstract. *In this work we adress the problem of structural and multi-functional shape and topology optimization using several elastic materials in a fixed working domain. The description and the evolution of the interfaces between the different phases is done using the level-set method. We use a smooth Hooke's tensor, instead of a discontinuous one. The continuous case can be seen as an approximation of the sharp interface case, and in this context, the signed distance function corresponding to each interface is used for modeling the smooth Hooke's tensor. A directional shape derivative is calculated for the objective function to minimize. We show 2d results for compliance minimization, as well as an example of multi-functional optimization, coupling structural and thermal problems.*

1 INTRODUCTION

Shape and topology optimization methods have become quite known among engineers and researchers during the last decades. They reduce significantly the amount of time needed for the design of a new mechanical part, help to optime existing designs, or even provide solutions to problems where intuition is very limited. Such a case is the optimal distribution of several materials, possibly having much different mechanical properties, in order to treat a multi-functionality criterion (e.g. stiffness and thermal isolation).

The modeling of a multi-material structure is usually done via a discontinuous Hooke's tensor. However, this choice can introduce severe complications in the numerical calculation of a shape derivative [2, 3, 8] and thus a smooth interpolation scheme is often preferable [3]. Moreover, a regularized Hooke's tensor seems to be more appropriate for some applications [14].

Many articles have been published on this topic in the framework of the SIMP (Solid Isotropic Material with Penalization) method (see [10, 11, 16] and the references therein). Several interpolation schemes have been proposed for the construction of the smooth Hooke's tensor and the penalization of intermediate densities. In the framework of the phase-field method for topology optimization, Zhou et al. [15] used a generalized Cahn-Hilliard model of multiphase transition to perform multimaterial structural optimization.

In the framework of the level set method for shape and topology optimization [1, 12], Mei et al. [5] and Wang et al. [13] were the first to present a regularized model for the Hooke's tensor using a multi-phase level-set method. In [3], Allaire et al. have used the same level-set representation and the signed-distance function to construct a smooth interpolation scheme for the Hooke's tensor. A directional shape derivative has been calculated and it has been shown that the problem converges to the one of sharp interface when the interpolation width tends to zero.

In this work, we adress the problem of structural and multi-functional shape and topology optimization. The same level-set representation and shape derivation as in [3] has been used. The method is first applied on a structural problem, where a single phase is substituted by two and three phases. Finally, a multi-functional problem is presented considering a structural and a thermal problem and two materials with much different mechanical properties.

2 SETTING OF THE PROBLEM

Without loss of generality, we limit ourselves with the description of the problem of compliance minimization using two materials. The extension to more phases is described in section 5.

We search to optimize the position of the interface Γ of two materials, 0 and 1, occupying two domains Ω^0 and Ω^1. Instead of assuming a sharp interface between the two materials, we work with a continuous and differentiable Hooke's tensor A. We assume that the material properties are smoothly interpolated in a region of width 2ϵ around the initial sharp interface, represented by the zero level set of a function ψ.

We introduce a working domain D (a bounded domain of $\mathbb{R}^d$, $(d = 2or3)$) which contains all admissible shapes, i.e. $\Omega^0 \cup \Omega 1 \subseteq D$. The volume and surface loads are given as two vector-valued functions defined on D, $f \in L^2(D)^d$ and $g \in H^1(D)^d$. The displacement field u is the

unique solution in $H^1(D)^d$ to the linearized elasticity system

$$\left\{\begin{array}{rcll} -\mathrm{div}\big(A(d_{\Omega^1}(x))\, e(u)\big) &=& f & \text{in } D \\ u &=& 0 & \text{on } \Gamma_D \\ \big(A(d_{\Omega^1}(x))\, e(u)\big)n &=& g & \text{on } \Gamma_N, \end{array}\right. \tag{1}$$

where $e(u)$ is the strain tensor, equal to the symmetrized gradient of u, $\Gamma_D \cup \Gamma_N \subset \partial D$ and $d_{\Omega^1}(x)$ is the signed-distance function to Ω^1.

We remind that if $\Omega \subset \mathbb{R}^d$ is a bounded domain, then the **signed distance function** to Ω is the function $\mathbb{R}^d \ni x \mapsto d_\Omega(x)$ defined by :

$$d_\Omega(x) = \left\{\begin{array}{ll} -d(x,\partial\Omega) & \text{if } x \in \Omega \\ 0 & \text{if } x \in \partial\Omega \\ d(x,\partial\Omega) & \text{if } x \in \overline{{}^c\Omega} \end{array}\right. , \tag{2}$$

where $d(\cdot,\partial\Omega)$ is the usual Euclidean distance.
The Hooke's tensor A is of the general form

$$A(d_\Omega(x)) = \left\{\begin{array}{lll} A_1 & ,if & d_\Omega(x) < -\epsilon, \\ f(d_\Omega(x)) & ,if & -\epsilon \le d_\Omega(x) \le +\epsilon, \\ A_0 & ,if & d_\Omega(x) > +\epsilon, \end{array}\right. \tag{3}$$

where $f(d_\Omega(x))$ is a smooth interpolation function. For example, a simple choice is to consider

$$A(d_\Omega(x)) = \left\{\begin{array}{lll} A_1 & ,if & d_\Omega(x) < -\epsilon, \\ \frac{A_1+A_0}{2} - \frac{(A_1-A_0)d_\Omega(x)}{2\epsilon} & & \\ -\frac{A_1-A_0}{2\pi} sin(\frac{\pi d_\Omega(x)}{\epsilon}) & ,if & -\epsilon \le d_\Omega(x) \le +\epsilon, \\ A_0 & ,if & d_\Omega(x) > +\epsilon. \end{array}\right. \tag{4}$$

Remark 2.1 *In 4 we have made a simple choice for the interpolation of the material properties between the two materials. Of course, one can choose any type of smooth interpolation. Moreover, the interpolation function can contain parameters that are also subject to optimization (f.e. the interpolation width ϵ) and a geometric and parametric optimization can be combined using a method of alternating directions.*

A classical choice for the objective function $J(\Omega)$ to be minimized is the compliance (the work done by the loads)

$$J(\Omega^1) = \int_D f \cdot u dx + \int_{\Gamma_N} g \cdot u ds = \int_D A(d_{\Omega^1}(x)) e(u) : e(u) dx. \tag{5}$$

3 SHAPE DERIVATIVE

In order to find a descent direction for advecting the shape, we compute a shape derivative for the objective function (5). The notion of the shape derivative dates back, at least, to Hadamard and there has been more contributions to its development. In this work, we follow the approach of Murat and Simon for shape derivation [6]. Starting from a smooth reference open set Ω, we consider domains of the type

$$\Omega_\theta = \big(Id + \theta\big)(\Omega),$$

with $\theta \in W^{1,\infty}(\mathbb{R}^d, \mathbb{R}^d)$. It is well known that, for sufficiently small θ, $(Id + \theta)$ is a diffeomorphism in $\mathbb{R}^d$.

Definition 3.1 *The shape derivative of $J(\Omega)$ at Ω is defined as the Fréchet derivative in $W^{1,\infty}(\mathbb{R}^d,\mathbb{R}^d)$ at 0 of the application $\theta \to J\big((Id+\theta)(\Omega)\big)$, i.e.*

$$J\big((Id+\theta)(\Omega)\big) = J(\Omega) + J'(\Omega)(\theta) + o(\theta) \quad \textit{with} \quad \lim_{\theta\to 0} \frac{|o(\theta)|}{\|\theta\|} = 0\ , \tag{6}$$

where $J'(\Omega)$ is a continuous linear form on $W^{1,\infty}(\mathbb{R}^d,\mathbb{R}^d)$.

Hadamard's structure theorem assures that the shape derivative of a functional can be written in the form

$$J'(\Omega)(\theta) = \int_{\partial\Omega} V(s)\theta(s)\cdot n(s)ds, \tag{7}$$

where V is the integrand of the shape derivative that depends on the specific objective function. Then, a descent direction can be found by advecting the shape in the direction $\theta(s) = -tV(s)n(s)$ for a small enough descent step $t>0$. For the new shape $\Omega_t = (\,\mathrm{Id}+t\theta)\,\Omega$, we can formally write

$$J\left(\Omega_t\right) = J\left(\Omega\right) - t\int_{\partial\Omega} V^2 ds + \mathcal{O}(t^2), \tag{8}$$

which guarantees a descent direction.

Remark 3.1 *A weaker notion of differentiability is that of the **directional derivative** of a functional $J(\Omega)$ at Ω in the direction $\theta\in V$, V being a banach space, which is defined as the limit in $\mathbb{R}$ (if it exists)*

$$J'(\Omega)(\theta) = \lim_{\delta\to 0} \frac{J((Id+\delta\theta)(\Omega)) - J(\Omega)}{\delta}. \tag{9}$$

Moreover, if the directional derivative at Ω exists for all $\theta\in\Omega$ and if $\theta\to J'(\Omega)(\theta)$ is a continuous linear application from V in $\mathbb{R}$, then we say that J is differentiable in the sense of Gâteaux at Ω.

The shape derivative of (5) has been calculated in [3] and we refer to this article for all technical details. The main difference with [5, 13] is that we calculate a shape derivative of the signed-distance function d_{Ω^1}, which should not be confused with the level-set function ψ used to describe and advect the shape, instead of performing variations of ψ.

Denoting $ray_\Gamma(x)\subset\mathbb{R}^d$ the set of points y such that d_{Ω^1} is differentiable at y, and whose projection on Γ is x ($p_\Gamma(y)=x$), κ_i ($i=1,...,d-1$) the principal curvatures of Γ at point $p_\Gamma(x)$, the shape derivative reads

$$J'(\Gamma)(\theta) = -\int_\Gamma \theta(x)\cdot n^1(x)[f_1(x)+f_0(x)]dx, \tag{10}$$

where

$$f_1(x) = \int_{ray_\Gamma(x)\cap\Omega^1} \frac{\partial A}{\partial d_{\Omega^1}} e(u):e(u) \prod_{i=1}^{d-1}(1+d_{\Omega^1}(s)\kappa_i(x))ds \tag{11}$$

and

$$f_0(x) = \int_{ray_\Gamma(x)\cap\Omega^0} \frac{\partial A}{\partial d_{\Omega^1}} e(u):e(u) \prod_{i=1}^{d-1}(1+d_{\Omega^1}(s)\kappa_i(x))ds. \tag{12}$$

A descent direction (a notion of a shape gradient) is then revealed as

$$\theta(x) = n^1(x)[f_1(x)+f_0(x)] \quad \forall x\in\Gamma.$$

4 LEVEL-SET REPRESENTATION

We favor an Eulerian approach and use the level-set method [7] to capture the subdomains Ω^0 and Ω^1 on a fixed mesh. Then, the boundary of Ω^0 and Ω^1 is defined by means of a level set function ψ such that (see Fig.(1))

$$\begin{cases} \psi(x) = 0 & \Leftrightarrow x \in \partial\Omega^0 \cap \partial\Omega^1 \cap D, \\ \psi(x) < 0 & \Leftrightarrow x \in \Omega^1, \\ \psi(x) > 0 & \Leftrightarrow x \in \Omega^0. \end{cases} \tag{13}$$

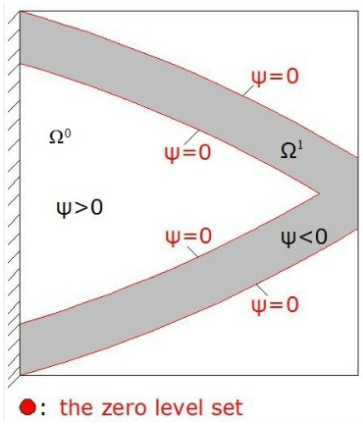

Figure 1: Level-set representation of the domains Ω^0 and Ω^1.

During the optimization process the shape is being advected with a velocity $V(x)$ derived from shape differentiation, as we will see in the sequel. The advection is described in the level-set framework by introducing a pseudo-time $t \in \mathbb{R}^+$ and solving the Hamilton-Jacobi equation

$$\frac{\partial \psi}{\partial t} + V|\nabla \psi| = 0, \tag{14}$$

using an explicit upwind scheme [9].

5 EXTENSION TO MORE THAN 2 MATERIALS

The method presented above can be easily extended to multi-materials (see also [13]). In fact, in order to represent m materials, we need $n = log_2 m$ level-set functions. To simplify the exposition we discuss the case of $m = 4$ phases which can be represented by two level set functions ψ_1 and ψ_0 corresponding to two "super-domains" O_1 and O_0 (see Fig.(2)).

More precisely, we define $\Omega^1 = O_1 \cap O_0^c$, $\Omega^2 = O_1^c \cap O_0$, $\Omega^3 = O_1 \cap O_0$, $\Omega^4 = O_1^c \cap O_0^c$, where O_i^c denotes the complementary of O_i. There are many ways of regularizing the Hooke's tensor A for this new problem. For example, one can use a regularized version of the Heaviside functions H_1 and H_0 of the super-domains O_1 and O_0, defined for $i = 0, 1$ as

$$H_i(d_i) = \begin{cases} 0 & if d_i < -\epsilon, \\ \frac{1}{2} + \frac{d_i}{2\epsilon} + \frac{1}{2\pi} sin(\frac{\pi d_i}{\epsilon}) & if -\epsilon \leq d_i \leq +\epsilon, \\ 1 & if d_i > +\epsilon, \end{cases}$$

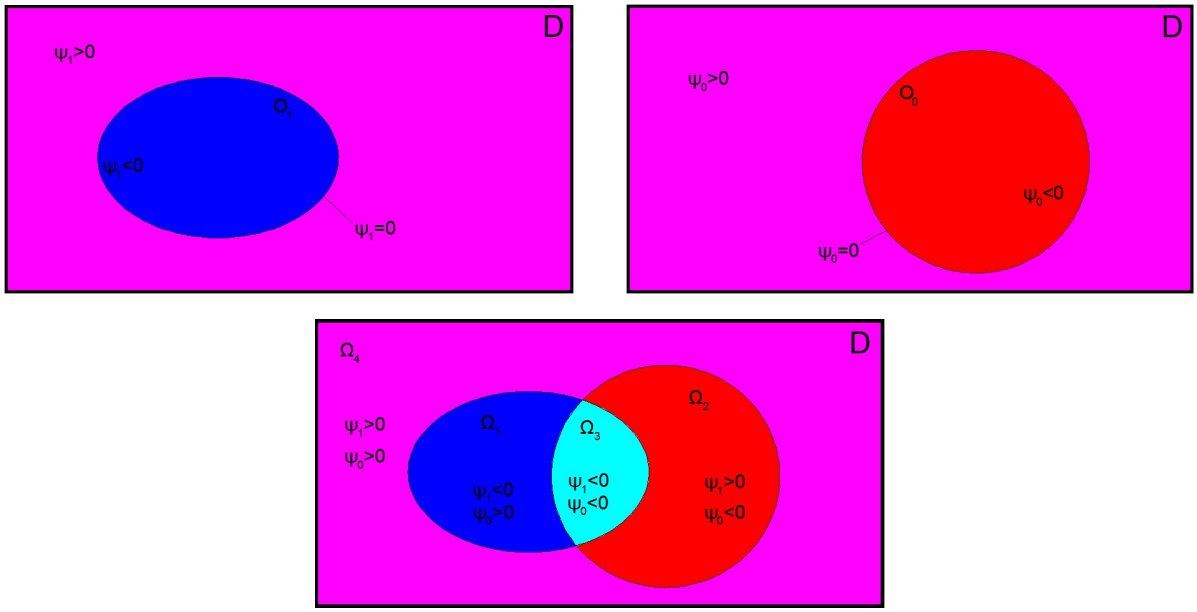

Figure 2: Two level-set functions defined on the same domain (top) and the four domains derived from combinations of their values (down).

where d_i is the signed-distance function to the super-domain O_i and then define the Hooke's tensor A as

$$\begin{aligned} A(d_1,d_0) &= +A_1(1-H_1(d_1))H_0(d_0) + A_2(1-H_0(d_0))H_1(d_1) \\ &\quad +A_3(1-H_1(d_1))(1-H_0(d_0)) + A_4H_0(d_0)H_1(d_1). \end{aligned}$$

Moreover, as the regularizing parameter $\epsilon \to 0$, the problem will converge to a problem of multi-materials with a sharp interface.
In this last case, the total compliance takes the form:

$$J(d_1,d_0) = \int_D A(d_1,d_0)e(u) : e(u). \tag{15}$$

We can consider two seperate vector fields θ_1 and θ_0 for the advection of the domains O_1 and O_0. Then, we caculate the shape derivative of the objective function (15) for each vector field separately and advect each of the domains O_1 and O_0 using their corresponding advection velocity (see [3]).

6 NUMERICAL RESULTS

6.1 Structural example

The first example is a 2×1 structure, clamped at the right and left part of its boundary and with a unit force applied at the middle of its lower part (see Fig.(3)). First, we minimize the compliance of the structure using one material with normalized Young modulus $E^1 = 1$, under the constraint $\int_\Omega dx = |D|/2$, where $|D|$ is the total volume of the domain D. The second material has $E^2 = eps << 1$ and simulates void. A simple augmented lagrangian algorithm is applied to enforce the volume constraint. The initialization and the optimized shape are shown in Fig.(4).

Suppose now that we want to replace half of this material with a weaker (but probably cheaper) material. In this case, we need to use three different phases, i.e. we need two

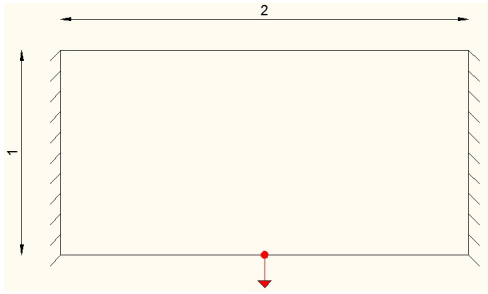

Figure 3: Boundary conditions.

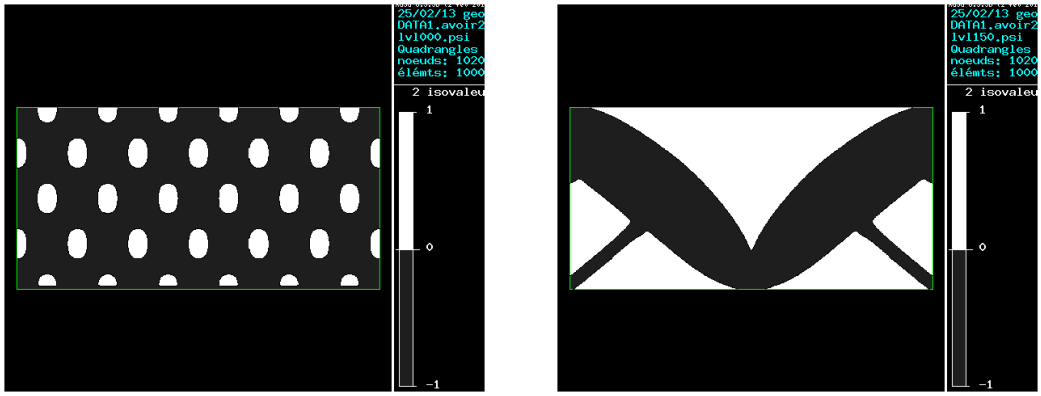

Figure 4: Initialization (left) and optimized shape (right) using one material.

level-set functions. Using two level-set functions we define four phases with Young modulus $E^1 = 1, E^2 = eps, E^3 = 0.5$ and $E^4 = eps$, i.e. materials $2, 4$ represent void. The volume constraints read now $\int_{\Omega^1} dx = |D|/4$ and $\int_{\Omega^3} dx = |D|/4$. The initialization and the optimized shape are shown in Fig.(5).

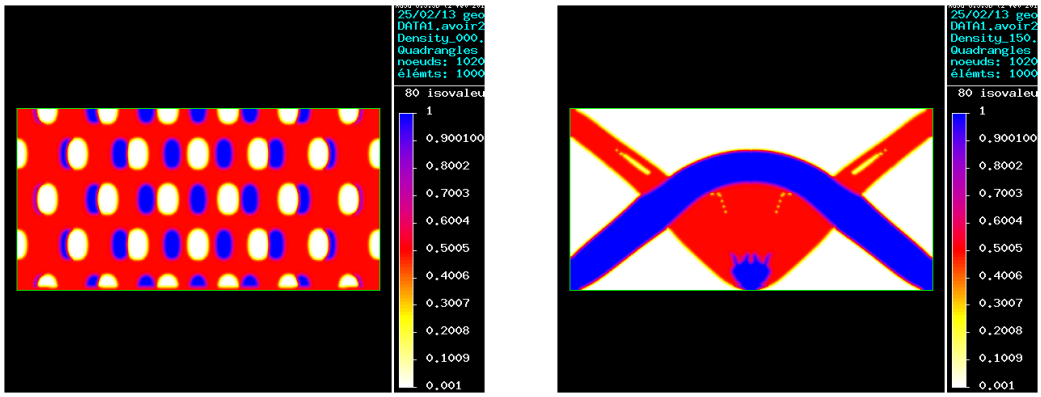

Figure 5: Initialization (left) and optimized shape (right) using two materials.

Using always two level-set functions we can optimize structures with up to three distinct phases and void. Choosing $E^1 = 1, E^2 = eps, E^3 = 0.7$ and $E^4 = 0.5$ and imposing $\int_{\Omega^1} dx = |D|/8$, $\int_{\Omega^3} dx = |D|/4$ and $\int_{\Omega^4} dx = |D|/8$, a local minimum is shown in Fig.(6).

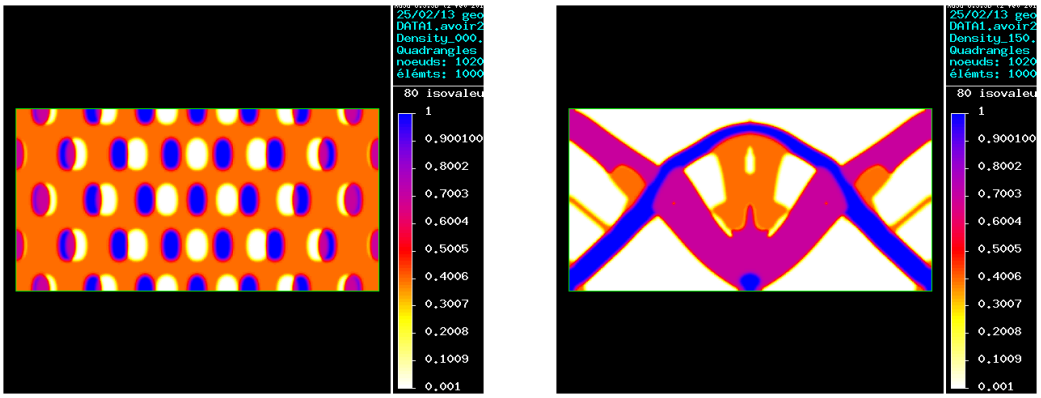

Figure 6: Initialization (left) and optimized shape (right) using three materials.

6.2 Multi-functional example

The second example couples a stuctural and a thermal problem. A 6×1 structure is considered (see Fig.(7)), having two non-optimizable areas (in blue) at the upper and lower part, occupied by material 1. The structure is subjected to two uncoupled mechanical problems. For the structural load case, the shape is considered clamped at its right and left boundary and a load is applied at the middle of the lower part. For the thermal load case, homogeneous Dirichlet conditions are considered for the lower part and the structure i subjected to a thermal flux either "in-plane" (Φ_2) or "out-of-plane" (Φ_1). The PDE describing the thermal problem reads

$$\left\{ \begin{array}{rcll} -\mathrm{div}\big(k(d_{\Omega^1}(x))\,\nabla T\big) &=& 0 & \text{in } D, \\ T &=& 0 & \text{on } \Gamma_D, \\ k(d_{\Omega^1}(x))\frac{\partial T}{\partial n} &=& \Phi_i & \text{on } \Gamma_N, \\ \frac{\partial T}{\partial n} &=& 0 & \text{on } \Gamma_0, \end{array} \right. \tag{16}$$

where $i = 1\, or\, 2$. Our goal is to distribute in an optimal way two materials with different properties, so as to create a structure that is stiff and thermally isolating at the same time. Material 1 has normalized Young modulus and thermal conductivity $E^1 = k^1 = 1$, while material 2 has $E^2 = k^2 = 0.1$, i.e. material 1 is stiffer but thermally more conductive than material 2.

As objective function to minimize, we will adopt the following choice presented in [4]

$$J(\Omega^1) = \frac{(\int_D A(d_{\Omega^1}(x))e(u)e(u)dx)^{1-a}}{(\int_D k(d_{\Omega^1}(x))\nabla T \cdot \nabla T dx)^a}, \quad a \in [0,1]. \tag{17}$$

The term in the nominator is the mechanical compliance, while the term in the denominator is the thermal compliance. The parameter "a" is chosen so as to highlight the importance of one or the other load case. For $a = 0$ the problems turns to the minimization of the mechanical compliance and thus all the optimisable area will be covered with the stiff material 1, while for $a = 1$ the problem is to minimize the thermal compliance, i.e. maximize the thermal isolation, and therefore the material 2 will be chosen. For intermediate values of "a", the algorithm will search for an optimal mixture of the two materials.

We consider both the case of "out-of-plane" and "in-plane" flux. The initialization for both cases is shown in Fig.(8). The optimized shape and the convergence diagram for "out-of-plane" flux and $a = 0.3$ is depicted in Fig.(9). In this figure we can see clearly that material 1 (in blue)

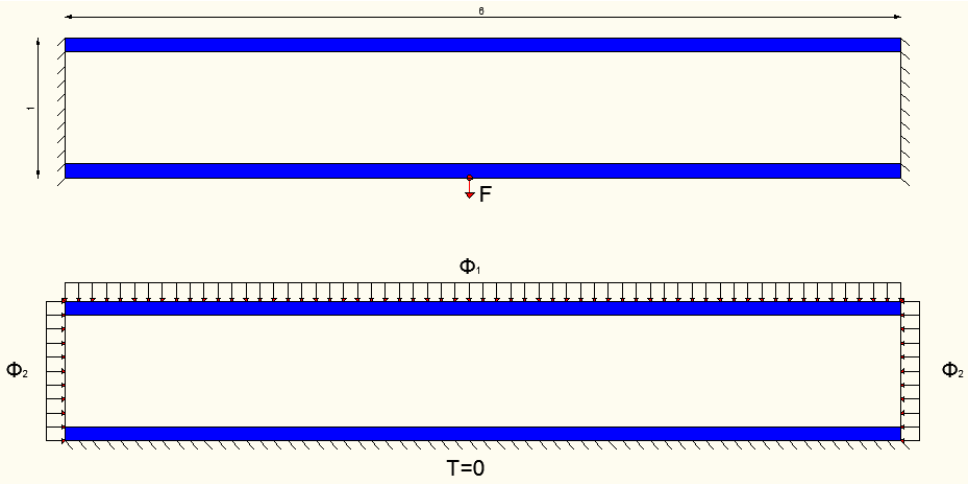

Figure 7: Boundary conditions."Out-of-plane" flux corresponds to $\Phi_1 \neq 0, \Phi_2 = 0$, while "in-plane" flux corresponds to $\Phi_2 \neq 0, \Phi_1 = 0$.

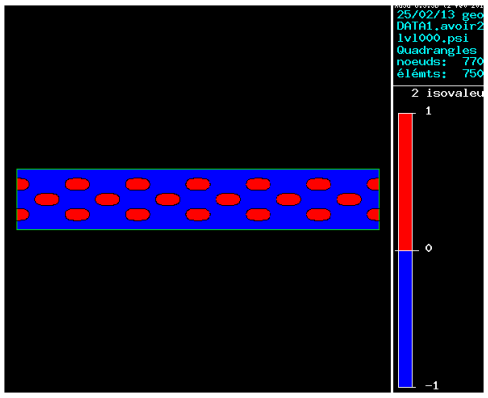

Figure 8: Initialization.

is placed so as to bear the structural load, whereas material 2 (in red) tries to prevent the thermal flux.

The case of "in-plane" flux is shown in Fig.(10) for $a = 0.5$. In this case, material 2 tries to isolate thermally the structure by being concentrated around the place that the flux is applied.

REFERENCES

[1] G. Allaire, F. Jouve and A.M. Toader, *Structural optimization using shape sensitivity analysis and a level-set method*, J. Comput. Phys., 194 (2004) pp. 363–393.

[2] G. Allaire, F. Jouve, N. Van Goethem, *Damage and fracture evolution in brittle materials by shape optimization methods,* J. Comp. Phys. 230, pp.5010-5044 (2011).

[3] G. Allaire, C. Dapogny, G. Delgado and G. Michailidis, *Multi-phase structural optimization via a level set method*, In preparation.

[4] L. Laszczyk, R. Dendievel, O. Bouaziz and Y. Bréchet, Optimisation des propriétés équivalentes de motifs périodiques: Cas d'un panneau architecturé en flexion, 10e colloque national en calcul des structures, 2011.

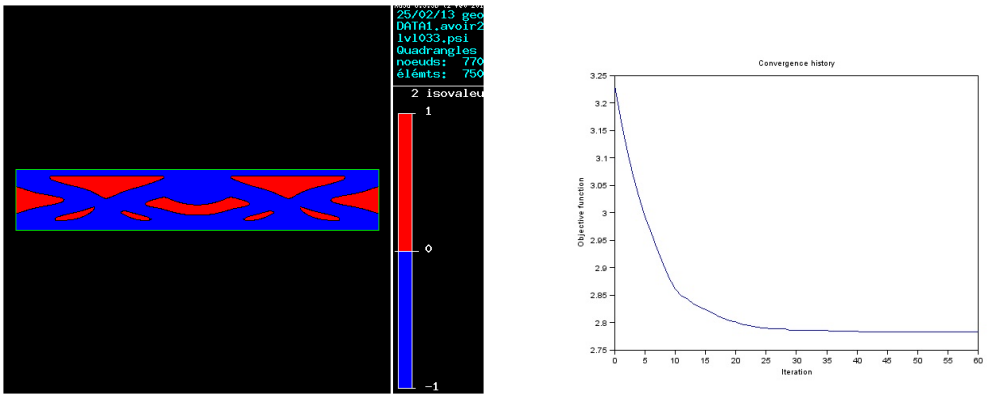

Figure 9: Optimized shape and convergence diagram for "out-of-plane" flux and $a = 0.3$.

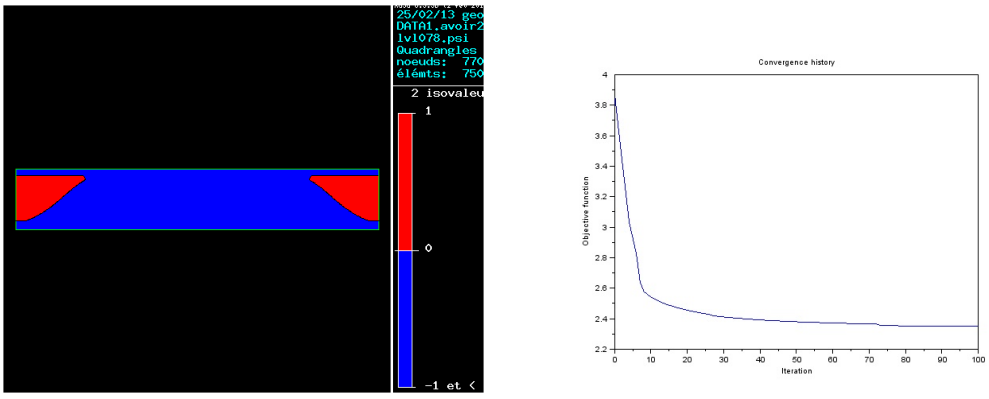

Figure 10: Optimized shape and convergence diagram for "in-plane" flux and $a = 0.5$.

[5] Y. Mei and X. Wang, *A level set method for structural topology optimization with multi-constraints and multi-materials,* ACTA MECHANICA SINICA, Vol.20, No.5, (2004).

[6] F. Murat and J. Simon, *Sur le contrôle par un domaine géométrique*, Technical Report RR-76015, Laboratoire d'Analyse Numérique (1976).

[7] S. Osher and J.A. Sethian, Front propagating with curvature dependent speed: algorithms based on Hamilton-Jacobi formulations. *J. Comp. Phys.* **78**, 12-49 (1988).

[8] O. Pantz, *Sensibilité de l'équation de la chaleur aux sauts de conductivité* C. R. Acad. Sci. Paris, Ser. I 341 (2005).

[9] J.A. Sethian, *Level-Set Methods and fast marching methods: evolving interfaces in computational geometry, fluid mechanics, computer vision and materials science,* Cambridge University Press (1999).

[10] O. Sigmund and S. Torquato, *Design of materials with extreme thermal expansion using a three-phase topology optimization method*, Journal of the Mechanics and Physics of Solids, 45(6):1037-1067 (1997).

[11] O. Sigmund, *Design of multiphysics actuators using topology optimization-part ii: Two-material structures*,Computer methods in applied mechanics and engineering, 190(49):6605-6627 (2001).

[12] M.Y. Wang, X. Wang and D. Guo, *A level-set method for structural topology optimization, Comput. Methods Appl. Mech. Engrg.*, **192**, 227-246 (2003).

[13] M. Wang and X. Wang, *Color level sets: a multi-phase method for structural topology optimization with multiple materials*, Comput. Methods Appl. Mech. Engrg. 193 (2004).

[14] N. Vermaak, G. Michailidis, Y. Brechet, G. Allaire, G. Parry and R. Estevez, *Material Interface Effects on the Topology Optimization of Multi-Phase Thermoelastic Structures Using A Level Set Method*, In preparation.

[15] S. Zhou and Q. Li, *Computational design of multi-phase microstructural materials for extremal conductivity*, Computational Materials Science, 43:549-564 (2008).

[16] S. Zhou and M.Y. Wang, *Multimaterial structural optimization with a generalized Cahn-Hilliard model of multiphase transition*, Struct Multidisc Optim, 33:89-111 (2007).